HAL
open science

Climate-mediated changes to mixed-layer properties in the Southern Ocean: assessing the phytoplankton response

P. W. Boyd, S. C. Doney, R. Strzepek, J. Dusenberry, K. Lindsay, I. Fung

To cite this version:

P. W. Boyd, S. C. Doney, R. Strzepek, J. Dusenberry, K. Lindsay, et al.. Climate-mediated changes to mixed-layer properties in the Southern Ocean: assessing the phytoplankton response. Biogeosciences Discussions, 2007, 4 (6), pp.4283-4322. hal-00297943

HAL Id: hal-00297943

https://hal.science/hal-00297943v1

Submitted on 18 Jun 2008

HAL is a multi-disciplinary open access archive for the deposit and dissemination of scientific research documents, whether they are published or not. The documents may come from teaching and research institutions in France or abroad, or from public or private research centers.

L'archive ouverte pluridisciplinaire **HAL**, est destinée au dépôt et à la diffusion de documents scientifiques de niveau recherche, publiés ou non, émanant des établissements d'enseignement et de recherche français ou étrangers, des laboratoires publics ou privés.

Biogeosciences Discuss., 4, 4283–4322, 2007
www.biogeosciences-discuss.net/4/4283/2007/
© Author(s) 2007. This work is licensed
under a Creative Commons License.

Biogeosciences Discussions

Biogeosciences Discussions is the access reviewed discussion forum of *Biogeosciences*

Climate-mediated changes to mixed-layer properties in the Southern Ocean: assessing the phytoplankton response

P. W. Boyd[1], S. C. Doney[2], R. Strzepek[1,3], J. Dusenberry[2], K. Lindsay[4], and I. Fung[5]

[1]NIWA Centre for Chemical and Physical Oceanography, Department of Chemistry, University of Otago, Dunedin, New Zealand
[2]Marine Chemistry and Geochemistry Department, Woods Hole Oceanographic Institution, Woods Hole, MA 02543 USA
[3]Department of Chemistry, University of Otago, Dunedin, New Zealand
[4]Climate and Global Dynamics, National Center for Atmospheric Research, Boulder, CO 80307 USA
[5]Department of Earth & Planetary Science, Berkeley Institute of the Environment, Berkeley, CA 94720-1250, USA

Received: 30 October 2007 – Accepted: 9 November 2007 – Published: 23 November 2007

Correspondence to: P. Boyd (pboyd@alkali.otago.ac.nz)

Abstract

Concurrent changes in ocean chemical and physical properties influence phytoplankton dynamics via alterations in carbonate chemistry, nutrient and trace metal inventories and upper ocean light environment. Using a fully coupled, global carbon-climate model (Climate System Model 1.4-carbon), we quantify anthropogenic climate change relative to the background natural interannual variability for the Southern Ocean over the period 2000 and 2100. Model results are interpreted using our understanding of the environmental control of phytoplankton growth rates – leading to two major findings. Firstly, comparison with results from phytoplankton perturbation experiments, in which environmental properties have been altered for key species (e.g., bloom formers), indicates that the predicted rates of change in oceanic properties over the next few decades are too subtle to be represented experimentally at present. Secondly, the rate of secular climate change will not exceed background natural variability, on seasonal to interannual time-scales, for at least several decades – which may not provide the prevailing conditions of change, i.e. constancy, needed for phytoplankton adaptation. Taken together, the relatively subtle environmental changes, due to climate change, may result in adaptation by resident phytoplankton, but not for several decades due to the confounding effects of climate variability. This presents major challenges for the detection and attribution of climate change effects on Southern Ocean phytoplankton. We advocate the development of multi-faceted tests/metrics that will reflect the relative plasticity of different phytoplankton functional groups and/or species to respond to changing ocean conditions.

1 Introduction

Climate change impacts ocean biota in many ways, and subsequently biological feedbacks may amplify or dampen any initial climate change signal (Denman et al., 1996; Boyd and Doney, 2003; Fung et al., 2005). These feedbacks arise from both changes

in bulk properties (primary production) and in floristics (e.g. diatoms versus coccolithophores) (Boyd and Doney, 2002). Coupled Ocean-Atmosphere Model (COAM) experiments indicate that ocean physical circulation and chemical properties will shift significantly in the coming decades (Sarmiento et al., 1998; Matear and Hirst, 1999). For the Southern (S.) Ocean, surface waters are projected to be warmer and fresher, with increased vertical stratification, shallower mixed-layer depths, reduced sea-ice, and higher oceanic CO_2 concentrations. Recent experiments indicate that S. Ocean westerly winds may increase in strength and shift poleward, increasing upwelling (Russell et al., 2006). Alteration of these upper ocean properties affect phytoplankton dynamics and growth rates directly and indirectly through modifications of vertical nutrient supply, mixed-layer depth, and light climate (Bopp et al., 2001).

Modeling studies have so far focused on simulating the decadal to centennial time-scale effects of climate change on phytoplankton processes, including the construction of biomes (Sarmiento et al., 2004), or the incorporation of more biological detail, such as algal functional groups (Iglesias-Rodriguez et al., 2002; Le Quéré et al., 2005; Litchman et al., 2006) or foodwebs (Legendre and Rivkin, 2005). Recent experimental approaches have concentrated on perturbation studies (weeks to months) on phytoplankton responses to light climate, CO_2 or nutrient concentrations, in laboratory cultures (Riebesell et al., 2000), shipboard experiments (Tortell et al., 2002), mesocosms (DeLille et al., 2005) or 50–200 km^2 in-situ patches of the ocean (Boyd et al., 2007).

Two steps are required to explore the relationship between climate-change mediated alteration of ocean properties and the consequent phytoplankton response on intermediary time-scales, i.e. decades – relevant to present experimental and observing system design and to policy makers (Dilling et al., 2003). First, models must provide estimates of future ocean environmental changes, and separate the effects of climate change from intrinsic interannual variability. Currently, COAM's provide one of the few plausible means to do this (Fung et al., 2005; Friedlingstein et al., 2006), and also offer the improved regional predictions needed to predict the rate of climate-mediated change in environmental properties for oceanic provinces.

Second, phytoplankton perturbation experiments must include realistic timescales for the alteration of environmental properties, quantify the potential for physiological plasticity or adaptability of organisms to climate perturbations, and investigate potential synergistic effects due concurrent changes in environmental drivers (e.g. iron and light). Initial experiments used large instantaneous perturbations (from 350 to 750 μatm CO_2, an IPCC climate-change scenario), resulting in altered calcification rates (Riebesell et al., 2000) or floristic shifts (Tortell et al., 2002). Such striking results represent an upper bound of the effects of climate-change mediated alterations in environmental forcing on phytoplankton processes. However, it is problematic to relate the results from such large, instantaneous perturbations, to the timescales and magnitude of climate change that phytoplankton will actually be exposed to. Phytoplankton can respond to environmental change from hours (e.g., algal photoacclimation, Falkowski and LaRoche, 1991), days/weeks (floristic shifts, Riebesell, 1991), to months/years (regime shifts, Boyd and Doney, 2003). This broad range of responses spans the transition from phytoplankton acclimation to adaptation (see Falkowski and LaRoche, 1991).

Here, we compare model estimates of the rates of change in ocean properties due to anthropogenic climate change with results from manipulation experiments, in which these properties have been altered for S. Ocean bloom-forming phytoplankton (i.e. we recognize the importance of climate effects on higher trophic levels but do not explore this topic here). Moreover, we examine the magnitude and sign of the S. Ocean climate-change and variability signatures, and discuss their implications for phytoplankton acclimation versus adaptation to environmental change. These results will inform us of whether the changes in upper ocean properties, and their impact on the biota, will be detectable over the coming decades, and how to design experiments to adequately represent these changes. If we can design such experiments, our findings will lead to improved attribution of the underlying natural and anthropogenic mechanisms driving such changes in the ocean, providing direct tests for the predictions made by numerical models used for future climate projections and policy decisions.

2 Methods and site selection

In this study, we focus on the S. Ocean – a region reported to have a disproportionately large impact on global climate (Sarmiento et al., 1998) and which is particularly sensitive to anthropogenic climate warming (e.g. Sarmiento et al., 2004). These waters are characterized by both high macronutrient concentrations (except for silicic acid in subpolar waters) and low rates of aerosol iron supply (Duce and Tindale, 1991; Fung et al., 2000). Macronutrient concentrations in polar waters are predicted to decrease by only ca. 10% due to climate change (Bopp et al., 2001) and thus the resident phytoplankton are unlikely to be subjected to macronutrient limitation.

Phytoplankton in large regions of the S. Ocean are iron-limited, and climate-change driven alterations of ocean physics will likely impact surface iron concentrations. It is not known whether regional dust deposition rates will increase or decrease due to climate change (Mahowald and Luo, 2003; Moore et al., 2006); likewise predictions of climate-mediated changes in UV irradiance are also inconclusive (Denman et al., 2007). Thus, the impact of changes in aerosol-iron supply or UV irradiance are not considered further here. In these waters, the biogeography of the key algal functional groups is already well defined, for example there are no nitrogen fixers in the S. Ocean (Westberry and Siegel, 2006), and a southwards decrease in coccolithophore abundance is observed (Cubillos et al., 2007).

2.1 Climate model formulation

Here, we utilize results from numerical climate simulations generated with the National Center for Atmospheric Research (NCAR) Community Climate System Model (CCSM) (Blackmon et al., 2001). The CSM1.4-carbon model is a fully coupled, global climate-carbon cycle simulation. The model formulation of this version and analyses of its pre-industrial equilibrium control solutions are detailed in Doney et al. (2006). The physical climate module consists of coupled atmosphere, land, ocean and ice components, and the exchanges between the model components conserve mass and energy. The

ocean and sea-ice model resolution are 3.6° in longitude and 0.8° to 1.8° latitude, with 25 levels in the vertical. The pre-industrial control solutions display stable surface climate and minimal deep ocean drift without requiring surface heat or freshwater flux adjustments. The water cycle is closed through a river runoff scheme.

Biogeochemistry in CSM1.4-carbon is simulated with modified versions of the terrestrial model CASA and the OCMIP-2 oceanic biogeochemistry model (Doney et al., 2004; Najjar et al., 2007). In the fully-coupled carbon-climate model, atmospheric CO_2 is a prognostic variable and is predicted as the residual after carbon exchanges with the land and ocean. The ocean biogeochemical component includes in simplified form the main processes for the solubility carbon pump, organic and inorganic biological carbon pumps, and air-sea CO_2 flux. The prognostic variables transported in the ocean model are phosphate, total dissolved inorganic, dissolved organic phosphorus, dissolved inorganic carbon, alkalinity, and oxygen.

New/export production is computed prognostically as a function of light, temperature, phosphate and iron concentrations. The maximum production as a function of temperature is multiplied by nutrient and light limitation terms. The nutrient term is the minimum of Michaelis-Menten limiting terms for PO_4 and Fe:

$$F_N = \min\{\frac{PO_4}{PO_4 + \kappa_{PO4}}, \frac{Fe}{Fe + \kappa_{Fe}}\} \quad (1)$$

where κ_{PO4} is 0.05 μmol/L and κ_{Fe} is 0.03 nmol/L. The light (irradiance) limitation term:

$$F_I = \frac{I}{I + \kappa_I}, \quad (2)$$

uses I, the solar short-wave irradiance, and a light limitation term κ_I (20 W/m^2). A fully dynamic iron cycle also has been added including atmospheric dust deposition/iron dissolution, biological uptake, vertical particle transport, and scavenging. In the simulations, as a simplification, dust deposited onto sea-ice is transferred directly to the ocean, with no modification to its properties, such as solubility (see Edwards and Sedwick, 2001).

2.2 21st century climate change experiments

A suite of transient experiments (1820–2100) branching off from the stable, pre-industrial control is conducted by specifying fossil fuel CO_2 emissions (Fung et al., 2005). A historical emission trajectory is used for the 19th and 20th centuries and the SRES-A2 "business-as-usual" fossil fuel emission scenario is used for the 21st century. No other greenhouse gases or radiative forcing perturbations are included. Carbon sources associated with anthropogenic land use modification are not included in these experiments. As the other radiative forcing nearly cancel in the 19th and 20th centuries, the climate simulation should be broadly comparable to that observed in the globally averaged sense. However, over the 19th and 20th centuries, land-use modification accounts for approximately 35% of the cumulative anthropogenic source of atmospheric CO_2. The simulated atmospheric CO_2 concentration in year 2000, therefore, is 20 ppmv too low compared to observations (~367 ppmv), lagging about 12 years behind reality. While the model CO_2 concentrations cannot be directly matched to calendar years, the overall CO_2 temporal trends for the 21st century and the year 2100 CO_2 concentration (~765 ppmv) are comparable to those from other carbon-climate projections (Friedlingstein et al., 2006).

The climate response for a particular variable χ, denoted as $\Delta\chi(t)$, is computed by differencing the transient climate and control simulations at a particular point in time t. The global mean surface air temperature increase $\Delta T_{air}(2100)$ is ~1.8 K. Friedlingstein et al. (2006) found that CSM1.4-carbon is at the lower end of reported climate sensitivities, $\Delta T_{air}/\Delta CO_2$, relative to several other coupled carbon-climate simulation. In benchmark studies, the transient climate response, i.e. temperature increase at the time of doubling of CO_2 where climate models are forced by a 1% y^{-1} increase in CO_2, is only 1.4 K for the NCAR CSM1.

Therefore, we have also conducted two additional experiments for the period 2000–2100 where we have artificially increased the climate sensitivity of the CSM1.4-carbon simulation to span the range observed in other COAM's. In these experiments, the

radiation calculations see a higher effective CO_2 concentration than seen by the land or ocean biogeochemistry. Specifically, radiative CO_2 is computed by calculating the perturbation in atmospheric CO_2 concentration above pre-industrial levels ΔCO_2, multiplying by factors of 2 and 4, respectively, and then adding back in the preindustrial concentration.

2.3 Climate change analysis

Climate warming influences marine ecology and biogeochemistry directly through temperature changes and indirectly through changes in ocean circulation (Boyd and Doney, 2003). The climate change signals in the S. Ocean of the CSM1.4-carbon simulation are approximately (though not exactly) zonal, and therefore we have partitioned the S. Ocean into polar and subpolar waters based on frontal structure, the boundary being set as the simulated 130 Sv streamfunction that approximates well the boundary between the two water masses. Annual time-series plots (model year 2000–2100) for key physical forcing factors and biogeochemical variables from the control and transient climate change simulations (A2, A2-2x, and A2-4x) are shown in Figs. 1 and 2 averaged over the polar and subpolar bands. Spatial maps of the temporal difference over 20 years (decade 2020–2029 minus 2000–2009) are shown in Fig. 3 for the same physical and biogeochemical properties.

Climate trends are significant only if they differ substantially from the drift of the control simulation, if non-zero, and are larger than the intrinsic interannual variability of the model. For the spatial maps, a Student's t-test is used to measure the significance of the differences between the two decades relative to the simulated interannual variability. Regions where $\Delta\chi$ (2020–2029 minus 2000–2009) is less than the standard error of χ for the decade 2000–2009 based on a student's t-test are masked out.

2.4 Phytoplankton perturbation experiments

Methods for laboratory culture experiments where light climate and/or trace metal concentrations were altered are presented in Appendix A. Due to the high ambient macronutrient concentrations in surface polar waters no macronutrient perturbation experiments were performed. For the methods used in other studies synthesized in Table 1b, please refer to these publications.

3 Results

3.1 Model simulations

The CSM1.4-carbon results are broadly similar to other COAM simulations that exhibit significant surface warming of S. Ocean waters in response to anthropogenic climate change. In the subtropical and subpolar regions, decadal mean sea surface temperature (SST) increases by 0.1–0.3 K/decade in the A2 case for a 20 year period (model years 2020–2029 minus 2000–2009) (Figs. 1–3; Table 1a). The A2 subpolar anthropogenic SST signal is significantly greater than the natural interannual variability for the region, even on this time-scale. The warming is less pronounced in polar waters closer to Antarctica in the A2 case; the temperature change does not exceed natural variability in most locations, and there is also a large area of cooling in the Atlantic sector. The anthropogenic temperature changes are even larger in the A2-x2 and A2-x4 climate sensitivity cases, and for the A2-x4 case the polar temperature rise becomes significant relative to natural variability.

Surface temperature is one of the few COAM variables for which we can compare the simulated surface ocean trends against the observed historical Southern Ocean record over the last several decades. This can be done due to the relatively large climate warming signal compared to interannual variability, and because of the relatively comprehensive in situ and satellite data coverage for temperature. But even for tem-

perature, the historical observation data set (particularly for subsurface waters) has significant gaps in the Southern Ocean, complicating model evaluation (Doney et al., 2007). Further, because the coupled model has its own internally-driven, non-linear climate variability that is often out of phase with the interannual variability of the real system, we are restricted to comparing long-term secular trends in the model and observations.

With those caveats in mind, the long-term spatial warming patterns in the model are broadly consistent with historical observations (Fig. 3). Like the model, observations exhibit higher surface warming in the Southern Ocean subtropical and subpolar bands than in polar waters, where there has either been no statistical trend or in some cases weak cooling rather than warming (Smith and Reynolds, 2005; Trenberth et al., 2007). Averaged zonally, the historical (1955–2003) upper ocean warming trends in the Southern Ocean are 0.0 to +0.025 K/decade for polar waters and +0.025 to +0.10 K/decade for subpolar waters (Levitus et al., 2005; Bindoff et al., 2007). Using subsurface float data from the 1990s relative to historical hydrography, Gille (2002) reports mid-depth (700–1000 m) warming rates of 0.04+/−0.01 K/decade averaged across 35 S to 65 S and rates as high as 0.08+/−0.02 K/decade in the core of the subantarctic front. The highest rates of subsurface ocean warming are comparable to the observational atmospheric surface warming rates for the Southern Ocean region of 0.13+/−.06 K/decade.

The CSM coupled model warming rates for the last half of 20th century (in model years 2000–2009 minus 1950–1959 adjusting for the atmospheric CO_2 delay) are in good agreement with the observed warming. As predicted by other coupled simulated, the model predicted warming rates tend to accelerate in the 21st century, with the simulated warming rates for the next 20 years of subpolar +0.10 to +0.31 K/decade; polar +0.03 to +0.17) (Figs. 1–3, Table 1).

The other clear anthropogenic signal is, as would be expected, the increase in surface water pCO_2 due to the rise in atmospheric CO_2 in the transient simulation. North of ~55° S, the ΔpCO_2 (here transient – control, not air – water) tracks the increase in the atmosphere, and values are 760–790 ppmv by 2100. Poleward of this boundary,

the surface water pCO_2 increases but not as rapidly as the atmosphere due to ice cover and the upwelling of older waters from below; average levels are only 720–760 ppmv by 2100.

For most of the other physical and biogeochemical factors in the CSM1.4 A2 case, however, the climate change signal is smaller than or comparable to natural variability on the decadal time-scale (2020–2029 minus 2000–2009), and there are spatial regions (sub-basin and basin scale) of both positive and negative change over twenty years. The anthropogenic climate change signals become more distinct in the A2-x2 and A2-x4 cases, with increased climate sensitivity, for the following properties: decreasing polar sea surface salinity, increased subpolar and polar stratification, decreased subpolar and polar surface dissolved iron concentrations, poleward shift and increased strength in polar upwelling, and increased polar surface ocean irradiance due to decreased ice fraction.

The climate response for surface phosphate and iron concentrations reflect the balance between changing upwelling and mixing of high nutrient, subsurface waters from below (source), residence time of surface water, and biological export production (sink). The rate of change of surface nutrient concentrations χ is given by:

$$\frac{\partial \chi}{\partial t} + \boldsymbol{u}_H \cdot \nabla_H \chi - \nabla_H K_H \nabla_H \chi + \boldsymbol{u}_Z \frac{\partial}{\partial z}\chi - \frac{\partial}{\partial z} K_Z \frac{\partial}{\partial z}\chi = \mathrm{RHS}_{\mathrm{bio}} \tag{3}$$

where the physical transport is partitioned into horizontal and vertical advection and mixing terms; the biological surface uptake and subsurface remineralization are grouped into a single biogeochemical right hand side term $\mathrm{RHS}_{\mathrm{bio}}$. Increased stratification and shallower mixed layers tend to decrease the mixing K_Z, while shifts in wind patterns may tend to increase upwelling u_Z while decreasing surface resident time-scales.

In CSM1.4, surface nutrient concentrations tend to stay constant or decrease. Phosphate exhibits a small decline from 40–60° S on average and is constant from 60° S to the pole. Phosphate concentrations remain large relative to κ_{PO4} and do not become limiting to organic matter production and export (Eq. 1). There are more notable

decreases in surface dissolved iron concentrations, −5 to −10 pmol/l relative to mean levels of 80–160 pmol/l for 40–60° S and −20 to −30 pmol/l relative to mean levels of 150–240 pmol/l south of 60° S. For comparison, the model half saturation constant for algal iron limitation for biological organic matter export κ_{Fe} is 30 pmol/l. The trends in surface macro- and micro-nutrients, along with the light/mixed layer and SST in turn impact the downward export flux (Eqs. 1 and 2). Integrated over the entire S. Ocean (including the subtropics), simulated organic matter export remains about the same, though it tends to shift poleward due to the southward migration in the band of deep winter mixing and the expansion of subtropical conditions. In the subpolar region, downward export increases by ∼10–15% in October and July while it tends to decrease further south.

The trends predicted for climate change of warmer waters, shallower mixed layers, and thus higher light levels, and lower nutrient and dissolved iron concentrations in the mixed layer (Table 1a) are consistent with the change in seasonal properties from spring to summer conditions (Table 2). The one exception to this is oceanic CO_2 concentrations, which are predicted to rise (Table 1a), akin to the progression from summer to winter conditions (Table 2). Together, the combination of the spring to summer progression (light, nutrients, metals) and summer to winter progression (CO_2) is something that phytoplankton will not have encountered previously. The seasonal amplitude in key oceanic properties in both polar and sub-polar waters is considerably greater than the magnitude of the predicted changes in these properties due to climate change (Table 1a c.f. Table 2), however there is insufficient resolution in the simulations to investigate how this seasonal amplitude will be influenced by climate change.

Broadly similar physical climate response patterns have been found in other 21st century coupled ocean-atmosphere climate simulations, though as mentioned above the CSM1.4-carbon model tends to be at the low end of the range in terms of climate sensitivity to atmospheric CO_2 perturbations. Using a series of empirical diagnostic calculations, Sarmiento et al. (2004) examined the potential marine ecological responses to climate warming using physical data from six different coupled climate model simu-

lations, including a variant of CSM 1. Averaged over the models, climate warming led to a contraction of the highly productive marginal sea ice biome and expansion of the subpolar gyre biome and low productivity, permanently stratified subtropical gyre biome in the S. Ocean. Vertical stratification tends to increase, which would be expected to decrease nutrient supply everywhere but also increase the growth season in some high latitude regions (Sarmiento et al., 2004). They did not investigate the magnitude of upwelling other than in defining the boundaries and shifts in biomes. Sarmiento et al. (2004) suggest that chlorophyll will increase in the open S. Ocean, due primarily to the retreat of and changes at the northern boundary of the marginal sea ice zone; but chlorophyll may tend to decrease adjacent to the Antarctic continent due primarily to freshening within the marginal sea ice zone. Estimated primary productivity generally will increase mainly as a result of warmer temperatures.

The climate-change driven trends in surface water properties in the S. Ocean do not occur independently, and synergistic effects need to be accounted for in phytoplankton responses. Table 3 presents property-property correlations for temperature, mixed layer depth and nutrient anomalies for both interannual variability (annual means from control simulation) and anthropogenic climate change (A2 case, decadal means of 2020-2029 minus 2000–2009; Fig. 3). For natural interannual variability, warmer SSTs are correlated with shallower mixed layers and lower surface nutrient concentrations; surface nutrients increase with mixed layer depth, and surface iron and phosphate are well correlated. The SST-surface nutrient correlations are of the same direction in the anthropogenic climate change case, although the magnitudes tend to differ from interannual variability. The correlations with mixed layer anomalies are weak and not statistically significant.

3.2 Polar phytoplankton responses to environmental perturbations

Physiological responses of both laboratory-cultured species and natural assemblages to altered environmental conditions are summarized (Table 1b). The range of conditions used in experiments (Table 1b) is readily compared to predicted changes in

these properties due to climate change (Table 1a). Tilzer et al. (1986) investigated temperature effects on photosynthetic performance in cells from the Scotia Sea and Bransfield Strait. Light-saturated photosynthesis ($P_b$max) increased significantly with increasing temperatures from −1.5°C to 8°C, c.f. Table 1a). The greatest enhancement of $P_b$max occurred between −1.5°C and 2°C (Q_{10}>4), but decreased at temperatures of >2 to 5°C, (Q_{10} of 2.6), and at >5°C was negligible. This response illustrates the high sensitivity of polar organisms to temperature (Clarke, 2003). Studies on coastal phytoplankton indicate that a 1°C–2°C warming around the Antarctic Peninsula might not alter photosynthetic rates, but could channel more photosynthate into DOC (Moran et al., 2006). Also in these waters, Moline et al. (2004) reported shifts from diatoms to chrysophytes, between 1991 and 1996, associated with warmer temperatures and a consequent reduction in salinity. Thus, warming can both directly and indirectly impact phytoplankton processes, and probably influences polar (ice melt, Q_{10}) more than sub-polar waters.

Natural gradients in surface nutrient concentrations (<5 to 45 μmol Si L^{-1}) such as during a southwards progressing bloom along the 170° W meridian (i.e. Pacific sector; Nelson et al., 2001) provides estimates of how the silicic acid uptake kinetics of diatoms are altered by changing upper ocean conditions. Such a lateral silicic acid gradient is much greater than the relative change in nutrient concentrations due to climate change (see PO_4, Table 1a). Nelson et al. (2001) observed no clear trend in affinity for silicic acid by diatoms (i.e. K_s) with latitude or silicic acid concentration, however there was an apparent seasonal progression – with a lower affinity for silicic acid evident over time. Critically, information in Nelson et al. (2001) on which species were present is lacking, and thus it is not known whether temporal/spatial shifts in floristics influenced these trends in uptake kinetics. Thus, their findings have limited value in predicting how diatoms, at the species level, might respond to predicted reductions in nutrient concentrations (Table 1a).

Manipulation of either light climate or CO_2 concentrations appear to have relatively little effect on polar species. Cultured phytoplankton can rapidly acclimate to a two-

to three-fold range of irradiances on a timescale of hours to days (R. Strzepek, unpublished data) Such photoacclimation has been widely reported for non-polar species (Falkowski and LaRoche, 1991). The maximum growth rate of *Phaeocystis antarctica* occurs at ~60 μmol quanta m^{-2} s^{-1} (Table 1b), and declines rapidly at lower irradiances, whereas at higher than saturating irradiances decreases in growth rate is much slower (R. Strzepek, unpublished data). This is also observed for cultured polar diatoms (R. Strzepek, unpublished data). Predictions in Table 1a indicate that increased mean irradiances, due to a shoaling of the mixed layer, will occur with climate change. However, this increase is probably too subtle to result in a detectable alteration of growth rates.

Beardall and Giordana (2002), reviewed phytoplankton CCM's (Carbon Concentrating Mechanisms), and suggest that rising ocean CO_2 concentrations may impact the performance of groups with (diatoms) and without (chrysophytes) CCM's. Rost et al. (2003) examined representative bloom-formers (diatom, coccolithophorid, and *Phaeocystis*) acclimated to 36–1800 ppmv CO_2. They reported major differences in each species ability to both regulate carbon acquisition and in the efficiency of acquisition. In the most comprehensive study of CCM's in S. Ocean biota to date, Tortell et al. (2007)[1] present evidence of the presence of inorganic CCM's (i.e. cells transporting HCO_3^- and utilizing carbonic anhydrase to catalyze HCO_3 dehydration to CO_2) for each of ten polar species, including *P. antarctica*, and *Fragilariopsis kerguelensis,* they investigated. This widespread presence of CCM's is evident for mixed assemblages in the subpolar Bering Sea (Martin et al., 2006) and NE Pacific (Tortell et al., 2006). Thus, it is difficult to predict whether any particular species would have a selective advantage to utilize CO_2 at the predicted higher concentrations (Table 1a).

In contrast to light climate and CO_2 concentrations, changes in dissolved iron concentrations had a pronounced effect on the growth rate (i.e. K_m, see Table 1b) of different polar species in culture, regardless of whether iron supply was expressed as

[1]Tortell, P. D., Rost, B., Strzepek, R., Boyd, P. W., and DiTullio, G.: Uptake and assimilation of inorganic carbon by Southern Ocean phytoplankton, Limnol. Oceanogr., submitted, 2007.

dissolved iron or bioavailable/free Fe (Table 1b). This range of dissolved iron concentrations (that set half the maximum algal growth rate) is considerably greater than predicted changes in dissolved iron concentrations due to climate change (Table 1a). Polar diatoms generally exhibited higher values of K_m than for *P. antarctica* (Table 1b), indicative of a greater sensitivity to future decreases in dissolved iron predicted by the model (Table 1a).

There are few studies of the synergistic effects due to simultaneous limitation (or its alleviation) of algal growth by multiple environmental factors. Takeda (1998) reported increased silicification rates at low, relative to high, dissolved iron concentrations in two cultured polar diatoms: silicification will be altered by both iron and silicic acid supply, two properties that will be influenced by climate change (Table 1a). Beardall and Giordano (2002) concluded that factors which may impact algal CCM's include CO_2 concentrations, temperature and also UV-B radiation. In SW Atlantic polar waters, Feller et al. (2001) reported that both SST and low dissolved iron concentrations limited growth rates of resident phytoplankton. These studies all point to the complex interactions between environmental properties that will be altered concurrently by climate change (Table 1a).

Other synergistic effects include iron and irradiance, and studies of iron/light interactions have reported up to threefold reductions in K_m for colonial *P. antarctica* following transfer from low to high light conditions (Sedwick et al., 2007; Table 1b). Strzepek (Table 1b) observed that, for three cultured *Thalassiosira* species and *P. antarctica* (non-colonial), the greatest effect of iron-limitation is observed at higher growth irradiances, i.e. μ/μmax is lower at higher light levels (where μ denotes Fe-limited and μmax represents Fe-replete growth rates). His findings differ from reports that low irradiance exacerbate algal iron requirements (Timmermans et al., 2001; Maldonado et al., 1999); this disparity may result from the use of different cultured species, or different methodologies (acclimated versus non-acclimated, i.e. Timmermans et al., 2001, cultures). Raven et al. (1999) suggest that low light results in both increases and decreases in algal iron requirements depending on species.

4 Discussion

4.1 Climate-change mediated alteration of ocean properties – response of the phytoplankton

Table 1a summarises the concurrent changes in factors that influence phytoplankton processes. The predicted decadal rates of change for all properties, including the largest climate change signal – CO_2 (3–4 ppmv yr^{-1}), are unprecedented on geological timescales (Denman et al., 2007); however they are small compared with experimental perturbations used to date (Table 1b). The studies, listed in Table 1b, provide valuable insights into what environmental factors control phytoplankton physiology. However, they will be of limited value for predicting the algal response to climate change, as they do not represent the potential for physiological plasticity and hence adaptation to the more gradual trends in environmental properties that will occur due to climate change. Such representation, for example, would require slow increases in CO_2 of 3–4 ppmv yr^{-1} for six months to several years. Such an experiment, albeit with a small change in CO_2, might permit extrapolation of the observed response of different species to perturbation, and would refine the approaches used previously (i.e. large instantaneous perturbations, Riebesell et al., 2000). But artifacts due to bottle or mesocosm containment will likely confound any biological response to the climate change signal. Thus, we must explore alternative means to capture, in some way, the effects of relatively slow rates of climate-mediated change on ocean properties.

Although the predicted rate of change in each ocean property is too subtle to be represented experimentally, it is possible that the potential multiplicative impact of synergistic effects (i.e. simultaneous limitation of algal growth by several factors) could be reproduced. Here, we consider iron and light. The model predicts lower dissolved iron concentrations and slightly higher underwater light levels (Table 1a), which may result, for some algal species (Raven et al., 1999), in greater iron and light co-limitation (i.e. the greatest displacement of growth rates from their maximum). It is also possible that cells may be growing faster (relative to the present day) due to the predicted

higher irradiances. However, any amplification of the biological signal due to a greater phytoplankton response to multiple factors (and their alteration by climate-change) may be countered by increased uncertainty, due to increased complexity, in predicting how phytoplankton dynamics will alter when multiple properties are considered. Therefore, the combined effect of simultaneous alteration of these factors is currently beyond prediction.

4.2 Climate change versus variability – implications for biological adaptation

In addition to climate change, other sources of variability will occur concurrently, including climate variability (e.g. SOI), seasonal gradients, and episodic (weeks) perturbations (e.g. dust storms). Although the effects of climate variability and climate change can be deconvolved in simulations (Fig. 3), these overlying effects will potentially confound the detection and attribution of trends in the biota as they respond to climate change. For the coming decades, the magnitude of change in oceanic properties due to climate variability is comparable to that by climate change, and moreover the direction of the change may differ between climate change and variability (Table 1a; see Sarmiento, 1993). Thus, it is possible that secular climate change will only induce significant biological effects when the magnitude of the environmental perturbations (and floristic changes) exceed background natural variability on seasonal to interannual time-scales. Such an inflection point might lead to detectable responses by the biota, as species commence selection for eco-types (Medlin, 1994) more suited to changing conditions where the sign of change is constant over time (i.e. adaptation rather than acclimation, Falkowski and LaRoche et al., 1991); as opposed to changing conditions with no prevailing trend due to fluctuations in the dominant control on the alteration of ocean properties (seasonal gradients, climate variability, climate change increase).

The assessment of the relative ability of different phytoplankton species to resist change and/or adapt to climate change may be a valuable tool to be used in conjunction with other experimental approaches such as Collins and Bell (2002). Resilience in phy-

toplankton, i.e. the maintenance of a given state when subject to disturbance (*sensu*, Carpenter and Cottingham, 1997), may result from an in-built tolerance of a wide range of environmental conditions (Margalef, 1978). Physiological plasticity, defined here as the ability to acclimate (i.e. physiological processes, Falkowski and LaRoche, 1991) to, and therefore gradually adapt (i.e. evolutionary processes, Falkowski and LaRoche, 1991) to, changing and/or new conditions, is akin to resilience. As stated earlier, such adaptation – over longer timescales – presupposes the need for a clear and sustained change in conditions. It is now established that oceanic organisms can adapt physiologically, over timescales of years, to pronounced environmental changes.

Such adaptability has been observed in corals, in response to warming temperature causing bleaching, which successfully responded by recruiting "new" algal symbionts (Baker et al., 2004). Furthermore, a thousand generations of *Clamydomonas* at elevated CO_2 concentrations resulted in smaller cell size and broader ranges in rates of photosynthesis and respiration (Collins and Bell, 2004). Thus, the relationship between the physiological plasticity of phytoplankton and the rate of change of environmental drivers is a key factor (and unknown) in determining whether such altered environmental forcing will result in floristic shifts and/or altered physiology.

There appears to be several key factors that control the degree of plasticity: a) the underlying survival strategy of organisms – specialist (k) or generalist (r) (Margalef, 1978); b) genetic variability and phytoplankton species and c) the timing of the emergence of different groups and/or species in the geological past. Generalist species tend to dominate in systems close to resource limitation such as oligotrophic waters (Reynolds, 1984). It is likely that the low iron supply, that characterises much of the S. Ocean, would favour r over k species, and the mandala of Margalef (1978) should be modified to include trace metals. Physiological plasticity will be driven by both geno- and pheno-typic characteristics, for example the success of bloom-forming phytoplankton may be due to their genetic variability, such that within-bloom genetic variability may be greater than that between blooms (Medlin et al., 1996). However little is known about whether genetic diversity between different species will result in a correspond-

ing degree of physiological or ecological "variability" (Iglesias-Rodriguez et al., 2006). The 2 year (i.e. 1000 generations) study of *Clamydomonas* by Collins and Bell (2004) presented evidence of accumulated mutations in genes affecting the CCM, after at elevated CO_2 concentrations, that were translated into physiological changes.

It is now evident that the physiological characteristics of different phytoplankton groups was strongly influenced by the ambient conditions when they emerged over time since the Proterozoic era. The trace metal requirements of different algal groups (high iron for diatoms) may have been set by the redox state of the ocean at the time of their emergence (Saito et al., 2003; Quigg et al., 2003; Falkowski et al., 2004). This may also be the case for coccolithophorids which evolved under different CO_2 conditions (Langer et al., 2006a). Experiments by Langer et al. (2006a, b) have shown that two species have different calcification responses across a range of CO_2 concentrations; *Coccolithus pelagicus* (no change with increasing CO_2 concentrations) and *Calcidiscus leptoporus* (maximum rate at present day CO_2 concentrations). Significantly, these responses differ from those reported by Riebesell et al. (2000) for *Emiliania huxleyi*. Thus, the ability to respond to changing trace metal or CO_2 conditions may have been imprinted during their evolutionary history.

4.3 Scenarios for phytoplankton responses – implications for detection versus attribution

Consideration of the possible effects of such physiological plasticity leads to three scenarios: 1) ecosystems are very "plastic" (Langer et al., 2006b)- with no or limited changes in community structure as the resident cells can adapt to climate change over years to decades; 2) the climate change signal simply results in a poleward migration of "fixed" biomes (Sarmiento et al., 2004); 3) conditions change sufficiently that a "new" community or ecosystem arises that has no analogue in current ocean (Boyd and Doney, 2003). These scenarios provide conceptual frameworks to examine the detection and attribution of such shifts.

Cells within "plastic" ecosystems could adjust their physiological properties rather

than alter species composition. Such a response is particularly difficult to detect and monitor, and would require a time-series of physiological experiments on natural populations. This approach has been advocated in terrestrial ecosystems, via the integration of observations on natural climate gradients with climate change experiments (Dunne et al., 2004). Climate-mediated shifts in biomes will probably be easier to detect and monitor, for example remote-sensing to monitor shifts in coccolithophore distributions was used successfully in the Bering Sea (Merico et al., 2003). Migration of the boundaries of biomes is less likely in the S. Ocean where the geographical isolation and strong meridional frontal boundaries (Smetacek and Nichol, 2005) minimize the impact of phenotypic adaptation (Medlin, 1994) and results in well-defined biomes. Thus, unanticipated floristic shifts will be conspicuous, and thus should be readily monitored.

In contrast, unanticipated shifts to a new assemblage, may not be readily detected, unless they have a different bio-optical signature that results in fortuitous detection by satellite sensors.

4.4 The magnitude of climate change versus the subsequent phytoplankton response

Our model predictions point to subtle changes in environmental properties that influence phytoplankton processes over the coming decades in the S. Ocean. How will such changes influence the response of the resident phytoplankton? Based on our limited knowledge, such as from long term time-series observations (Smayda et al., 2005), or case studies of the effects of climate variability (Chavez et al., 1999), adaptation is the most likely algal response to climate change in these waters (N.B. this does not take into account top-down foodweb effects). The extension of biomes is unlikely due to the strong circumpolar features in the S. Ocean and the magnitude of change in oceanic properties is probably insufficient in the next two decades to result in pronounced floristic shifts. Such dramatic shifts, for example from low picophytoplankton stocks to diatom blooms, are mediated by climate variability in the Equatorial Pacific (Chavez et al., 1999), but are driven by large and rapid changes in environmental conditions (i.e. a sixfold increase in vertical iron supply between years, c.f. Table 1a). As

such they are generally poor proxies for climate change. However, such adaptation to climate change, and its detection, in the next twenty years will be confounded by other sources of climate variability.

4.5 Approaches to investigate phytoplankton responses to climate change

No single approach is sufficient to address this pressing issue. Due to the difficulties in conducting manipulation experiments which represent the predicted rates of change in oceanic properties, multi-faceted tests for assessment of change should be developed (e.g. Peterson and Keister (2003). A nested suite of perturbation experiments including laboratory (mechanistic understanding of physiological pathways; see MacIntyre and Cullen, 2005) and shipboard experiments (physiology of assemblages), mesocosms or mesoscale perturbations (floristic shifts and their underlying mechanisms), and novel ecosystem modeling techniques (Follows et al., 2007) are required. Climate-change perturbation studies in terrestrial systems reveal the major influence of experimental duration (up to 5 years) on the outcome of perturbation (Walther, 2007), but extrapolating such conclusions to the ocean is problematic due to differences in the turnover of plant biomass between land (years) and ocean (days) (Falkowski et al., 1998).

Boyd and Doney (2002) advocated the use of perturbation experiments, monitoring and biogeography to investigate the effects of climate change and the subsequent feedbacks. Their approach required both global (incorporation of greater biological complexity) and regional (data interpretation based on a scheme of provinces). Our study provides further insights into what degree of biological complexity is required. The use of evolutionary history in conjunction with assessment of the paleo-environment under which algal groups emerged is a powerful tool to interpret the results from perturbation experiments (Langer et al., 2006a, b). Thus, the three-stranded approach of Boyd and Doney (2002) must also incorporate a nested suite of perturbations, and information on phytoplankton plasticity.

Appendix A

Algal manipulation experiments – culturing techniques

Lab culture experiments – using recent isolates (2004) from HNLC S. Ocean which have been maintained in low metal media – key algal species include bloom forming diatoms such as *Fragilariopsis kerguelensis*, *Chaetoceros* spp., *Proboscia alata*, and the other key bloom former in the open Southern Ocean – *Phaeocystis antarctica*. *P. antarctica* was isolated in the austral summer of 2001 at 61° 20.8′ S, 139° 50.6′ E from a single colony. The culture was rendered axenic by treatment with antibiotics (Cottrell and Suttle, 1993), which was confirmed by epifluorescent microscopy on culture subsamples treated with DAPI according the recommendation of Kepner and Pratt (1994).

Phytoplankton were grown in the artificial seawater medium Aquil (Price et al., 1988) prepared in Milli-Q water (Millipore Corp.). The seawater, containing the major salts, was enriched with 10 μmol L^{-1} phosphate, 100 μmol L^{-1} silicate and 300 μmol L^{-1} nitrate. Trace metal contaminants were removed from the medium and nutrient enrichment stock solutions using Chelex 100 ion exchange resin (Sigma, St. Louis, MO) according to the procedure of (Price et al., 1988). Media were enriched with filter-sterilized (0.2 μm Gelman Acrodisc PF) EDTA-trace metal and ESAW vitamin solutions (Harrison et al., 1980). Free trace metal ion concentrations, in the presence of 10 μmol L^{-1} EDTA as the chelating agent, were as follows (-log free metal ion concentration = pMetal): pCu 13.79, pMn 8.27, pZn 10.88, and pCo 10.88. These concentrations were calculated using the chemical equilibrium computer program MINEQL (Westall et al., 1976) with the thermodynamic constants reported in Ringbom (1963) . Selenite and molybdate were added at 10^{-8} and 10^{-7} mol L^{-1} respectively. The salinity and initial pH of the medium was 35 psu and 8.17±0.04 (n=13), respectively. All cultureware and plastics that came in contact with cultures were rigorously cleaned and sterilized according to the procedures detailed in Maldonado and Price (1996) to

minimize trace metal and bacterial contamination. Media were prepared and cultures were sampled in a sterile Class 100 laminar flow bench.

Solitary cells of *P. antarctica* were grown in semi-continuous batch cultures at 4±1°C in continuous light at 7 intensities (3, 20, 30, 60, 100, 400 and 570 μmol photons $m^{-2}\,s^{-1}$) obtained using fluorescent bulbs (12 W Sylvania) attenuated with neutral density screening, and measured with a 4π quantum meter (model QSL-2101, Biospherical Instruments, San Diego, CA). The basal medium contained 1.8±0.1 nmol L^{-1} iron contamination (n=6), which was determined electrochemically (*CLE-ACSV,* competitive ligand equilibrium- adsorptive cathodic stripping voltammetry). At each growth irradiance, cultures were grown in a variety of media that differed in their total Fe concentration, and Fe-organic complex type and concentration. High iron medium was prepared by adding 2.6 nmol L^{-1} of pre-mixed, filter-sterilized FeEDTA (1:1) which, due to the photolability of FeEDTA complexes, corresponds to a range of measured inorganic iron concentrations ([Fe$\prime$]=53–111 pmol L^{-1} from 3 to 570 μmol photons $m^{-2}\,s^{-1}$) as determined with the sulfoxine method. Cultures were also grown in Aquil medium containing either 10 or 100 μmol L^{-1} of EDTA containing and no added iron. To induce Fe stress, 2 nmol L^{-1} of Fe was added as a complex with 4, 40 or 400 nmol L^{-1} of the terrestrial siderophore desferrioxamine B mesylate (DFB, Sigma) to Aquil medium containing 10 μmol L^{-1} of EDTA to chelate the other trace metals. Stock DFB solutions (0.1–10 mmol L^{-1}) were prepared in Milli-Q water, and were 0.2 μm filter sterilized after dissolution. The Fe was premixed with the DFB before addition to the media as previously described (Maldonado and Price, 1999). The media with the added FeDFB complex were allowed to equilibrate overnight. As *P. antarctica* maintained maximum growth rates in Aquil medium containing no added Fe and either 10 or 100 μmol L^{-1} of EDTA, we assumed that the 1.8 nmol L^{-1} Fe contamination in the basal medium was bioavailable. Therefore the FeDFB ratios in these media were 3.8:4, 3.8:10, and 3.8:100 nmol L^{-1}, respectively.

Specific growth rates (d^{-1}) were calculated from least-squares regressions of ln in vivo fluorescence versus time during the exponential growth phase of acclimated cul-

tures. During experiments to explore the physiological plasticity of *Fragilariopsis kerguelensis*, *Proboscia alata*, and *P. antarctica* to iron availability and light climate, Fe treatments ranging from 19.4 to Fe:DFB 4:400 nM, Growth PFD from 5 to 400 mol photons $m^{-2} s^{-1}$.

Acknowledgements. Philippe Tortell (UBC) kindly provided unpublished data from a recently submitted manuscript. S. C. Doney was supported in part by the WHOI Ocean and Climate Change Institute. Computational resources were provided by the NCAR Climate Simulation Laboratory. The National Center for Atmospheric Research is sponsored by the U.S. National Science Foundation. P. Boyd was supported by the NZ FRST Coasts and Oceans OBI.

References

Arrigo, K. R., Robinson, D. H., Worthen, D. L., Dunbar, R. B., DiTullio, G. R., VanWoert, M., and Lizotte, M. P.: Phytoplankton community structure and the drawdown of nutrients and CO_2 in the Southern Ocean, Science, 283, 365–367, 1999.

Baker, A. C., Starger, C. J., McClanahan, T. R., and Glynn, P. W.: Corals' adaptive response to climate change, Nature, 430, 741, 2004.

Beardall, J. and Giordano, M.: Ecological implications of microalgal and cyanobacterial CO_2 concentrating mechanisms, and their regulation, Funct. Plant Biol., 29, 335–347, 2002.

Bindoff, N.L., Willebrand, J., Artale, V., Cazenave, A., Gregory, J., Gulev, S., Hanawa, K., Le Quéré, C., Levitus, S., Nojiri, Y., Shum, C.K., Talley L.D., and Unnikrishnan A.: Observations: Oceanic Climate Change and Sea Level, in: Climate Change 2007: The Physical Science Basis, Contribution of Working Group I to the Fourth Assessment Report of the Intergovernmental Panel on Climate Change, edited by: Solomon, S., Qin, D., Manning, M., Chen, Z., Marquis, M., Averyt, K. B., Tignor, M. and Miller, H. L., Cambridge University Press, Cambridge, United Kingdom and New York, NY, USA, 2007.

Blackmon, M., Boville, B., Bryan, F., Dickinson, R., Gent,P., Kiehl, K., Moritz, R., Randall, D., Shukla, J., Solomon, S., Bonan, G., Doney, S., Fung, I., Hack, J., Hunke, E., Hurrell, J., Kutzbach, J., Meehl, J., Otto-Bliesner, B., Saravanan, R., Schneider, E.K., Sloan, L., Spall, M., Taylor, K., Tribbia J., and Washington, W.: The Community Climate System Model, Bull. Amer. Meteorol. Soc., 82, 2357–2376, 2001.

Bopp, L., Monfray, P., Aumont, O., Dufresne, J.-L., Le Treut, H., Madec, G., Terray L., and Orr, J. C.: Potential impact of climate change on marine export production, Global Biogeochem. Cy. 15, 81–99, 2001.

Boyd, P. W. and Doney, S. C.: Modelling regional responses by marine pelagic ecosystems to global climate change, Geophys. Res. Lett., 29(16), 53-1 to 53-4, doi:10.1029/2001GL014130, 2002.

Boyd, P. and Doney, S. C.: The impact of climate change and feedback process on the ocean carbon cycle, in: Ocean Biogeochemistry, edited by: Fasham, M., Springer, 157–193, 2003.

Boyd, P. W., Law, C. S., Hutchins, D. A., Abraham, E. R., Croot, P. L., Ellwood, M., Frew, R. D., Hadfield, M., Hall, J., Handy, S., Hare, C., Higgins, J., Hill, P., Hunter, K. A., LeBlanc, K., Maldonado, M. T., McKay, R. M., Mioni, C., Oliver, M., Pickmere, S., Pinkerton, M., Safi, K., Sander, S., Sanudo-Wilhelmy, S. A., Smith, M., Strzepek, R., Tovar-Sanchez, A., and Wilhelm, S. W.: FeCycle: Attempting an iron biogeochemical budget from a mesoscale SF 6 tracer experiment in unperturbed low iron waters, Global Biogeochem. Cy., 19, GB4S20, doi:10.1029/2005GB002494, 2005.

Boyd, P. W., Jickells, T., Law, C. S., Blain, S., Boyle, E. A., Buesseler, K. O., Coale, K. H., Cullen, J. J., de Baar, H. J. W., Follows, M., Harvey, M., Lancelot, C., Levasseur, M., Owens, N. P. J., Pollard, R., Rivkin, R. B., Sarmiento, J., Schoemann, V. Smetacek, V., Takeda, S., Tsuda, A., Turner, S., and Watson, A. J.: Mesoscale iron enrichment experiments 1993–2005: Synthesis and future directions, Science, 315, 612–617, 2007.

Carpenter, S. R. and Cottingham, K. L.: Resilience and restoration of lakes, Conservation Ecology (online): 2, available from the Internet: http://www.consecol.org/vol1/iss1/art2/, 1997

Clarke, A.: Costs and consequences of evolutionary temperature adaptation, Trends Ecol. Evol., 18, 573–581, 2003.

Cloern, J. E., Grenz, C., and L. Vidergar-Lucas, L.: An empirical model of the phytoplankton chlorophyll : carbon ratio-the conversion factor between productivity and growth rate, Limnol. Oceanogr., 40, 1313–1321, 1995.

Collins, S. and Bell, G.: Phenotypic consequences of 1000 generations of selection at elevated CO_2 in a green alga, Nature, 431, 566–569, 2004.

Cottrell, M. T. and Suttle, C. A.: Production of Axenic Cultures of Micromonas-Pusilla (Prasinophyceae) Using Antibiotics, J. Phycol., 29, 385–387, 1993.

Cubillos, J. C., Wright, S. W., Nash, G., de Salas, M. F., Griffiths, B., Tilbrook, B., Poisson, A., and Hallegraeff, G. M.: Shifts in geographic distributions of calcification morphotypes of

the coccolithophorid Emiliania huxleyi in the Southern Ocean during 2001–2006, Mar. Ecol. Prog. Ser., 348, 47–58, 2007.

DeLille, B., Harlay, J., Zondervan, I., Jacquet, S., Chou, L., Wollast, R., Bellerby, R. G. J., Frankignoulle, M., Borges, A. V., Riebesell, U., and Gattuso, J. P.: Response of primary production and calcification to changes of pCO_2 during experimental blooms of the coccolithophorid Emiliania huxleyi, Global Biogeochem. Cy., 19, GB2023, doi:10.1029/2004GB002318, 2005.

Denman, K., Hofmann, E., and Marchant, H.: Marine biotic responses and feedbacks to environmental change and feedbacks to climate, in: Climate Change 1995, edited by: Houghton, J. T., Meira Filho, L. G., Callander, B. A., et al., The Science of Climate Change, Cambridge University Press, 1996.

Denman, K. L., Brasseur, G., Chidthaisong, A., Ciais, P., Cox, P. M., Dickinson, R. E.,Hauglustaine, D., Heinze, C., Holland, E., Jacob, D., Lohmann, U., Ramachandran, S., da Silva Dias, P. L., Wofsy S. C., and Zhang, X.: Couplings Between Changes in the Climate System and Biogeochemistry, in: Climate Change 2007: The Physical Science Basis. Contribution of Working Group I to the Fourth Assessment Report of the Intergovernmental Panel on Climate Change, edited by: Solomon, S., Qin, D., Manning, M., Chen, Z., Marquis, M., Averyt, K. B., Tignor, M., and Mille, H. L., Cambridge University Press, Cambridge, UK, 2007.

Dilling, L., Doney, S. C., Edmonds, J., Gurney, K. R., Harriss, R., Schimel, D., Stephens, B., and Stokes, G.: The role of carbon cycle observations and knowledge in carbon management, Ann. Rev. Env. Resour., 28, 521–558, doi:10.1146/annurev.energy.28.011503.163443, 2003.

Doney, S. C., Bullister, J. L., and Wanninkhof, R.: Climatic variability in upper ocean ventilation diagnosed using chlorofluorocarbons, Geophys. Res. Lett., 25, 1399–1402, 1998.

Doney, S. C., Lindsay, K., Caldeira, K., Campin, J.-M., Drange, H., Dutay, J.-C., Follows, M., Gao, Y., Gnanadesikan, A., Gruber, N., Ishida, A., Joos, F., Madec, G., Maier-Reimer, E., Marshall, J. C., Matear, R. J., Monfray, P., Mouchet, A., Najjar, R., Orr, J. C., Plattner, G.-K., Sarmiento, J., Schlitzer, R., Slater, R., Totterdell, I. J., Weirig, M.-F., Yamanaka, Y., and Yool, A.: Evaluating global ocean carbon models: the importance of realistic physics, Global Biogeochem. Cy., 18, GB3017, doi:10.1029/2003GB002150, 2004.

Doney, S. C., Lindsay, K., Fung I., and John, J.: Natural variability in a stable 1000 year coupled climate-carbon cycle simulation, J. Climate, 19, 3033–3054, 2006.

Doney, S. C., Yeager, S., Danabasoglu, G., Large, W. G., and McWilliams, J. C.: Mechanisms governing interannual variability of upper ocean temperature in a global hindcast simulation, J. Phys. Oceanogr., 37, 1918–1938, 2007.
Duce, R. A. and Tindale, N. W.: The atmospheric transport of iron and its deposition in the ocean, Limnol. Oceanogr., 36, 1715–1726, 1991.
Dunne, J. A., Saleska, S. R., Fischer, M. L., and Harte, J.: Integrating experimental and gradient methods in ecological climate change research, Ecology, 85 904–916, 2004.
Edwards, R. and Sedwick, P.: Iron in East Antarctic snow: Implications for atmospheric iron deposition and algal production in Antarctic waters. Geophys. Res. Lett., 28, 3907-3910, 2001.
Falkowski, P. G. and LaRoche, J.: Acclimation to spectral irradiance in algae, J. Phycol., 27, 8–14, 1991.
Falkowski P. G., Barber, R. T., and V. Smetacek, V.: Biogeochemical controls and feedbacks on ocean primary production, Science, 281, 200–206, 1998.
Falkowski, P. G., Katz, M. E., Knoll, A. H., Quigg, A., Raven, J. A., Schofield, O., and Taylor, F. J. R.: The Evolution of Modern Eukaryotic Phytoplankton, Science 305, 354, doi:10.1126/science.1095964, 2004.
Feller, G., Ellis-Evans, J. C., Deubert, C., and Connelly, D. P.: Regulation by low temperature of phytoplankton growth and nutrient uptake in the Southern ocean, Mar. Ecol. Prog. Ser., 219, 51–64, 2001.
Follows, M. J., Dutkiewicz S., Grant, S., and Chisholm, S. W.: Emergent Biogeography of Microbial Communities in a Model Ocean, Science, 1843–1846, 2007.
Friedlingstein, P., Cox, P., Betts, R., Bopp, L., von Bloh, W., Brovkin, V., Cadule, S. Doney, M. Eby, I. Fung, G. Bala, J. John, C. Jones, F. Joos, T. Kato, P., Kawamiya, M., Knorr, W., Lindsay, K., Matthews, H. D., Raddatz, T., Rayner, P., Reick, C., Roeckner, E., Schnitzler, K.-G., Schnur, R., Strassmann, K., Weaver, A. J., Yoshikawa, C., and Zeng, N.: Climate–carbon cycle feedback analysis: Results from the C4MIP model intercomparison, J. Climate, 19(14), 3337–3353, 2006.
Fung, I. Y., Meyn, S. K., Tegen, I., Doney, S. C., John, J. G., and Bishop, J. K. B.: Iron supply and demand in the upper ocean, Global Biogeochem. Cy., 14, 697–700, 2000.
Fung, I., Doney, S. C., Lindsay, K., and John, J.: Evolution of carbon sinks in a changing climate, Proc. Nat. Acad. Sci. (USA), 102, 11 201–11 206, doi:10.1073/pnas.050494910, 2005.
Gille, S. T.: Warming of the Southern Ocean since the 1950s. Science, 295, 5558, 1275–1277,

2002.
Gordon, L. I., Codispoti, L. A., Jennings, J. C., Millero, F. J., Morrison, J. M., and Sweeney, C.: Seasonal evolution of hydrographic properties in the Ross Sea, Antarctica, 1996–1997, Deep Sea Res. II, 47, 3095–311, 2000.
Harrison, P. J., Waters, R. E., and Taylor, F. J. R.: A broad spectrum artificial seawater medium for coastal and open ocean phytoplankton, J. Phycol., 16, 28–35, 1980.
Hiscock, M. R., Marra, J., Smith, W. O., Barber, R. T.: Primary productivity and its regulation in the Pacific Sector of the Southern Ocean, Deep Sea Res. II, 50, 533–558, 2001.
Iglesias-Rodriguez, M. D., Brown, C. W., Doney, S. C., Kleypas, J., Kolber, D., Kolber, Z., Hayes, P. K., and Falkowski, P. G.: Representing key phytoplankton functional groups in ocean carbon cycle models: coccolithophores, Global Biogeochem. Cycles, 16, 1100, doi:10.1029/2001GB001454, 2002.
Iglesias-Rodriguez, M. D., Schofield, O. M., Batley, J., Medlin L. K., and Hayes, P. K.: Intraspecific genetic diversity in the marine coccolithophore Emiliania huxleyi (Prymnesiophyceae): The use of microsatellite analysis in marine phytoplankton population studies, J. Phycol. 42, 526–536, 2006.
Kepner, R. L. and Pratt, J. R.: Use of Fluorochromes for Direct Enumeration of Total Bacteria in Environmental-Samples – Past and Present, Microbiol. Rev. 58, 603–15, 1994.
Langer G., Geisen, M., Baumann, K.-H, Klaus, J., Riebesell, U., Thoms, S., and Young, J. R.: The response of Calcidiscus leptoporus and Coccolithus pelagicus to changing carbonate chemistry of seawater, Geophys. Res. Abst., 8, 05161, 2006a.
Langer G., Geisen M., Baumann K.-H., Klaus, J., Riebesell, U., Thoms, S., and Young, J. R.: Species-specific responses of calcifying algae to changing seawater carbonate chemistry, Geochem. Geophys. Geosyst., 7, Q09006, doi:10.1029/2005GC001227, 2006b.
Legendre L. and Rivkin, R. B.: Integrating functional diversity, food web processes, and biogeochemical carbon fluxes into a conceptual approach for modeling the upper ocean in a high-CO 2 world, J. Geophys. Res., 110, C09S17, doi:10.1029/2004JC002530, 2005.
Le Quéré C., Harrison, S. P., Prentice, C., Buitenhuis, E. T., Aumont, O., Bopp, L., Claustre, H., Cotrim Da Cunha, L., Geider, R., Giraud, X., Klaas, C., Kohfeld, K., Legendre, L., Manizza, M., Platt, T., Rivkin, R. B., Sathyendranath, S., Uitz, J., Watson, A. J., and Wolf-Gladrow, D.: Ecosystem dynamics based on phytoplankton functional types for global ocean biogeochemistry models, Global Change Biol. 11, 2016–2040, 2005.
Levitus, S., Antonov, J. I., and Boyer, T. P: Warming of the World Ocean, 1955–2003, Geophys.

Res. Lett., 32, L02604, doi:10.1029/2004GL021592, 2005.
Litchman, E., Klausmeier, C. A., Miller, J. R., Schofield, O. M., and Falkowski, P. G.: Multi-nutrient, multi-group model of present and future oceanic phytoplankton communities, Biogeosciences, 3, 585–606, 2006, http://www.biogeosciences.net/3/585/2006/.
MacIntyre, H. L. and Cullen, J. J.: Using cultures to investigate the Physiological ecology of Microalgae, in: Algal Culturing Techniques, edited by: Andersen, R. A., Elsevier, Amsterdam, 287–326, 2005.
Mahowald, N. M. and Luo, C.: A less dusty future?, Geophys. Res. Lett., 30(17), 1903, doi:10.1029/2003GL017880, 2003.
Mahowald, N. M., Baker, A. R., Bergametti, G., Brooks, N., Duce, R. A., Jickells, T. D., Kubilay, N., Prospero, J. M., and Tegen, I.: Atmospheric global dust cycle and iron inputs to the ocean, Global Biogeochem. Cy., 19, GB4025, doi:10.1029/2004GB002402, 2005.
Maldonado, M. T. and Price, N. M.:. Influence of N substrate on Fe requirements of marine centric diatoms, Mar. Ecol. Prog. Ser, 141, 161–172, 1996.
Maldonado, M. T. and Price, N. M.: Utilization of iron bound to strong organic ligands by plankton communities in the subarctic Pacific Ocean. Deep-Sea Res. II, 46, 2447–2473, 1999.
Margalef, R: Life-forms of phytoplankton as survival alternatives in an unstable environment, Oceanologia Acta, 1, 493–509, 1978.
Martin, C. L. and Tortell, P. D.: Bicarbonate transport and extracellular carbonic anhydrase activity in Bering Sea phytoplankton assemblages: Results from isotope disequilibrium experiments, Limnol. Oceanogr. 51, 2111–2121, 2006.
Matear, R. and Hirst, A. C.: Climate change feedback on the future oceanic CO_2 uptake. Tellus 51, 722–733, 1999.
Measures C. I. and Vink, S.: Dissolved Fe in the upper waters of the Pacific sector of the Southern Ocean, Deep Sea Res. II, 48, 3913–3941, 2001.
Medlin, L. K.: Genetic Variability and phytoplankton species, Chapter 34, IOC Workshop report # 142, 257–265, 1994.
Medlin, L. K., Barker, G. L. A., Wrieden, S., and Vaulot, D.: Genetic characterisation of Emiliania huxleyi (Haptophyta), J. Mar. Syst., 9, 13–31, 1996.
Merico, A., Tyrrell, T., Brown, C. W., Groom, S. B., and Miller, P. I.: Analysis of satellite imagery *for* Emiliania huxleyi blooms in the Bering Sea before 1997, Geophys. Res. Lett., 30, 1337–1340, 2003.

Moline, M. A., Claustre, H., Frazer, T. K., Schofield, O., and Vernet, M.: Alteration of the food web along the Antarctic Peninsula in response to a regional warming trend, Global Change Biol., 10, 1973–1980, doi:10.1111/j.1365-2486.2004.00825, 2004.

Moran, X. A. G., Sebastián, M., Pedros-Alio, C., and Estrada, M.: Response of Southern ocean phytoplankton and bacterioplankton production to short-term experimental warming, Limnol. Oceanogr. 51, 1791–1800, 2006.

Najjar, R. G., Jin, X., Louanchi, F., Aumont, O., Caldeira, K., Doney, S. C., Dutay, J.-C., Follows, M., Gruber, N., Joos, F., Lindsay, K., Maier-Reimer, E., Matear, R. J., Matsumoto, K., Monfray, P., Mouchet, A., Orr, J. C., Plattner, G. K., Sarmiento, J. L., Schlitzer, R., Slater, R.D., Weirig, M.-F., Yamanaka, Y., and Yool,A.: Impact of circulation on export production, dissolved organic matter and dissolved oxygen in the ocean: Results from Phase II of the Ocean Carbon-cycle Model Intercomparison Project (OCMIP-2), Global Biogeochem. Cy., 21, GB3007, doi:10.1029/2006GB002857, 2007

Nelson, D. M., Brzezinski, M. A., Sigmon, D. E., and Franck, V. M.: A seasonal progression of Si limitation in the Pacific sector of the Southern Ocean, Deep-Sea Res. II, 48, 3973–3995, 2001.

Nodder, S. D., Boyd, P. W., Chiswell, S. M., Pinkerton, M. H., Bradford-Grieve, J. M., Greig, M. J. N.: Temporal coupling between surface and deep ocean biogeochemical processes in contrasting subtropical and subantarctic water masses, southwest Pacific Ocean, J. Geophys. Res., 110, C12017, doi:10.1029/2004JC002833, 2005.

Peterson, W. T. and Keister, J. E.: Interannual variability in copepod community composition at a coastal station in the northern California Current: A multivariate approach, Deep-Sea Res. II, 50, 2499–2517, 2003.

Price, N. M., Harrison, G. I., Hering, J. G., Hudson, R. J., Nirel, P. M. V., Palenik, B., and Morel, F. M. M.: Preparation and chemistry of the artificial algal culture medium Aquil, Biol. Oceanogr., 6, 443–461, 1988.

Quigg, A., Finkel, Z. V., Milligan, A. J., Wyman, K., Falkowski, P. G., and Morel, F. M. M.: The evolutionary inheritance of elemental stoichiometry in marine phytoplankton, Nature, 425, 291–294, 2003.

Raven, J. A., Evans, M. C. W., and Korb, R. E.: The role of trace metals in photosynthetic electron transport in O_2-evolving organisms, Photosynth. Res., 60, 111–149, 1999.

Reynolds, C. S.: The Ecology of Freshwater Phytoplankton, 397 pp., Cambridge University Press, Cambridge, UK, 1984.

Riebesell, U. Zondervan, I., Rost, B., Tortell, P. D., Zeebe, R. E., and Morel, F. M. M.: Reduced calcification of marine plankton in response to increased atmospheric CO_2, Nature, 407, 364–367, 2000.
Ringbom, A.: Complexation in Analytical Chemistry. New York: Interscience, 1963.
Rost, B., Riebesell, U., and Burkhardt, S.: Carbon acquisition of bloom-forming marine phytoplankton, Limnol. Oceanogr., 48, 55–67, 2003
Russell, J. L., Dixon, K. W., Gnanadesikan, A., Stouffer, R. J., and Toggweiler, J. R.: The Southern Hemisphere westerlies in a warming world: propping open the door to the deep ocean, J. Climate, 19, 6382–6390, 2006.
Saito, M. A., Sigman, D. M., and Morel, F. M. M: The bioinorganic chemistry of the ancient ocean: the co-evolution of cyanobacterial metal requirements and biogeochemical cycles at the Archean-Proterozoic boundary?, Inorg. Chim. Acta, 356, 308–318, 2003.
Sarmiento, J. L.: Atmospheric CO_2 stalled, Nature, 365, 697–698, 1993.
Sarmiento, J. L., Hughes, T. M. C., Stouffer, R. J., and Manabe, S.: Simulated response of the ocean carbon cycle to anthropogenic climate warming, Nature, 393, 245–249, 1998.
Sarmiento, J. L., Slater, R. Barber, R., Bopp, L., Doney, S. C., Hirst, A. C., Kleypas, J., Matear, R., Mikolajewicz, U., Monfray, P., Soldatov, V., Spall, S. A., and Stouffe, R.: Response of ocean ecosystems to climate warming, Global Biogeochem. Cy., 18, GB3003, doi:10.1029/2003GB002134, 2004.
Sedwick, P. N., Garcia, N. S., Riseman, S. F., Marsay, C. M., and DiTullio, G. R.: Evidence for high iron requirements of colonial Phaeocystis antarctica at low irradiance, Biogeochemistry, 83, 83–97, doi:10.1007/s10533-007-9081-7, 2007.
Sherlock, V., Pickmere, S., Currie, K., Hadfield, M., Nodder, S., and Boyd, P. W.: Predictive accuracy of temperature-nitrate relationships for the oceanic mixed layer of the New Zealand region, J. Geophys. Res., 112, C06010, doi:10.1029/2006JC003562, 2007.
Smayda, T. J., Borkman, D. G., Beaugrand, G., and Belgrano, A. G.: Ecological effects of climate variation in the North Atlantic: Phytoplankton, in: Ecological Effects of Climatic Variations in the North Atlantic, edited by: Stenseth, N. C., Ottersen, G., Hurrell, J., and Belgrano, A., Oxford Univ. Press., UK, 48–58, 2005.
Smetacek, V. and Nichol, S.: Polar ocean ecosystems in a changing world, Nature, 437, 362–368, 2005.
Smith, T. M. and Reynolds, R. W.: A global merged land and sea surface temperature reconstruction based on historical observations (1880–1997), J. Climate, 18, 2021–2036, 2005.

Takeda, S.: Influence of iron availability on nutrient consumption ratio of diatoms in oceanic waters, Nature, 393, 774–777, 1998.

Tilzer, M. M., Elbrächter, M., Gieskes, W. W., and Beese, B.: Light-Temperature interactions in the control of photosynthesis in Antarctica phytoplankton, Polar Biol., 5, 105–111, 1986.

Timmermans, K. R., Gerringa, L. J. A., de Baar, H. J. W., van der Wagt, B., Veldhuis, M. J. W., de Jong, J. T. M., and Croot, P. L.: Growth rates of large and small Southern ocean diatoms in relation to the availability of iron in natural seawater, Limnol. Oceanogr., 46, 260–266, 2001.

Tortell, P. D., DiTullio, G. R., Sigman, D. M. and Morel, F. M. M.: CO_2 effects on taxonomic composition and nutrient utilization in an Equatorial Pacific phytoplankton assemblage, Mar. Ecol. Progr. Ser., 236, 37–43, 2002.

Tortell, P. D., Martin and C. L., and Corkum, M. E.: Inorganic carbon uptake and intracellular assimilation by subarctic Pacific phytoplankton assemblages, Limnol. Oceanogr. 51, 2102–2110, 2006.

Trenberth, K. E., Jones, P. D., Ambenje, P., Bojariu, R., Easterling, D., Klein, A., Tank, T., Parker, D., Rahimzadeh, F., Renwick, J. A., Rusticucci, M., Soden, B., and Zhai, P.:Observations: Surface and Atmospheric Climate Change, in: Climate Change 2007: The Physical Science Basis, Contribution of Working Group I to the Fourth Assessment Report of the Intergovernmental Panel on Climate Change, edited by: Solomon, S., Qin, D., Manning, M., Chen, Z., Marquis, M., Averyt, K. B., Tignor, M., and Miller, H. L., Cambridge University Press, Cambridge, United Kingdom and New York, NY, USA, 2007.

Walther, G.-R.: Tackling ecological complexity in climate impact research, Science, 315, 606–607, 2007.

Westall, J. C., Zachary, J. L., and Morel, F. M. M.: MINEQL: A computer program for the calculation of chemical equilibrium composition of aqueous systems, (Department of Civil engineering, MIT, Cambridge, Massachusetts), 1976.

Westberry, T. K. and Siegel, D. A.: Spatial and temporal distribution of Trichodesmium blooms in the world's oceans, Global Biogeochem. Cy., 20, GB4016, doi:10.1029/2005GB002673, 2006.

Table 1. Comparison for S. Ocean sub-polar and polar waters of the relative rate of a) climate-change mediated alteration of annual-mean ocean properties that influence phytoplankton processes expressed as change per decade compared with; b) A summary of the range of conditions for each ocean property under which manipulation experiments have been conducted on either key polar bloom-forming species, or natural polar assemblages. The climate change rates in a) are estimated from a suite of fully coupled CSM 1.4-Carbon simulations by spatially averaging over the subpolar or polar domains (boundary defined by the 130 Sv stream function contour) and averaging over the period 2000 and 2100. The model ranges correspond with the simulations with varying model climate sensitivities to atmospheric CO_2 perturbations. The model estimated rms variability in annual-mean, spatial averaged ocean properties due to natural climate variability is included for reference. nd denotes uncertainty over sign of change (Mahowald et al., 2005). Due to the paucity of data on sub-polar phytoplankton this summary focuses only on polar waters.

a)

Property	Rate of change Subpolar waters per decade	Rate of Change Polar waters per decade 1	RMS variability for subpolar waters due to natural climate variability	RMS variability for polar waters due to natural climate variability
Temperature deg. C	+0.10 to +0.31	+0.03 to +0.17	0.11	0.13
Salinity psu	−.003 to −.007	−.014 to −.042	0.017	0.027
Mixed layer depth m	+0.3 to −0.8	−0.3 to −0.8	3.0	2.0
Stratification $kg/m^4 \times 10^{-4}$	+0.16 to +0.67	+0.28 to +1.49	0.94	0.77
Surface PO4 μmol/l	−.001 to −.005	+.001 to −.004	.012	0.012
Surface Fe nmol/l$\times 10^{-3}$	−0.32 to −1.30	−1.89 to −5.58	1.80	3.85
pCO_2 ppmv	+33.9 to +44.6	+37.4 to +41.0	0.8	1.2
Light climate	Surf. PAR 0.03 to 0.05 W/m^2 Water column PAR$ 0.004 to 0.006 W/m^2	Surface PAR 0.02 to 0.23 W/m^2 Water column PAR$ 0.003 to 0.005 W/m^2	Surface PAR 0.49 W/m^2 Water column PAR$ 0.04 to 0.05 W/m^2	Surface PAR 0.43 W/m^2 Water column PAR$ 0.05 to 0.07 W/m^2
Aerosol dust	nd	nd	nd	nd
Ice fraction	−.0003 to −.0004	−.003 to −.013	0.0015	0.013

$ surface mixed-layer light climate was derived using mixed layer depth and chlorophyll concentration (as a proxy of light attenuance) as detailed in Boyd et al. (2007).

1 W/m^2 ~0.4 mol quanta $m^{-2}\,d^{-1}$ from Cloern et al. (1995).

Table 1. Continued.

b) Polar waters				
Property	*Phaeocystis antarctica*	*Fragillariopsis kerguelenis*	*Proboscia alata*	Diatom species or natural populations
Temperature	No data	No data	No data	See text Natural populations@
Nutrient supply (Si)	Non-siliceous+	No data	No data	See text Diatom bloom#
Dissolved iron (DFe) Iron bioavailability (Fe')## CO_2 Light climate	K_m=0.1 nMˆ 0.32 aM–25.4 fM CCM present Rapid photo-acclimation (hours 40–400 μmol quanta m^{-1} s^{-1})	K_m=0.57$ 3.5 aM to 0.27 pM CCM present Rapid photo-acclimation	No data 0.64 aM to 51.3 fM CCM present Rapid photo-acclimation	K_m=0.006 to >1 nM$ 3.5 aM to 0.27 pM& CCM* See text Rapid photo-acclimation
Dissolved iron and light climate	K_m decreased from 0.35 nM Fe at low light to 0.1 nM at high lightˆ μmax (i.e. Fe replete) at 60 μE	See text	See text	Low light results in both increases and decreases in Fe requirements depending on spp. (Raven et al., 1999)
Other synergistic effects a) Temperature and light b) Light and CCM's c) Temperature and Fe supply	No data	No data	No data	See text, (Tilzer et al., 1986) See text, Beardall and Giordana (2002) See text, natural populations, Feller et al. (2001)

@ Tilzer et al. (1986), Scotia Sea and Bransfield Strait, light-saturated and light-limited photosynthetic rates and their relationship with temperature.

+ altered N:P ratios for *P. antarctica* relative to diatoms (more efficient N uptake per unit P (Arrigo et al., 1998).

Nelson et al. (2001) study of silica uptake kinetics along a meridional gradient in silicic acid ranging from <5 in the north to 45 μM in the South.

ˆ Sedwick et al. (2007), effects of iron and light on the growth of natural populations of colonial *Phaeocystis antarctica*, Ross Sea

$ Timmermans et al. (2001), K_m (dissolved iron concentration versus growth rate (DFe for $^1/_2$ μmax)) for a range of diatoms including *Chaetoceros brevis* (K_m 0.006) to *Actinocyclus* (1.14),

Timmermans et al. (2001) used dissolved iron as they could not define Fe bioavailability, and we have used Fe' as a proxy for bioavailability.

& lab culture studies on Southern Ocean polar isolate *Eucampia Antarctica* (R. Strzepek, unpublished data)

* CCM's denote the presence of an inorganic Carbon Concentrating Mechanism. All polar species so far examined (9 diatoms and *P. antarctica*) have all exhibited CCM's (Tortell et al., 2007[1]).

Table 2. Summary of seasonal ranges for a) the polar waters of the Ross Sea; and b) for subpolar waters S of New Zealand (i.e. S of the STF and N of the SAF).

a) polar waters		
Mixed layer Property	Seasonal range	Reference
Incident irradiance	6–56 mol quanta m^{-2} d^{-1}	Hiscock et al. (2001)
Mixed layer depth	<40 m to >100 m	Measures and Vink (2001)
Nitrate	34 to <20 μmol L^{-1}	Gordon et al. (2000)
Silicic acid	74 to 66 μmol L^{-1}	Gordon et al. (2000)
tCO_2	2140 to 2260 μmol Kg^{-1}	Gordon et al. (2000)
Dissolved iron	0.22 to 0.1 nmol L^{-1}	Measures and Vink (2001)
b) subpolar waters		
Mixed layer Property	Seasonal range	Reference
Incident irradiance	13–45 mol quanta m^{-2} d^{-1}	Boyd (unpublished data)
Mixed layer depth	<30 m to >120 m	Nodder et al. (2005)
Nitrate	15 to <6 μmol L^{-1}	Sherlock et al. (2006)
Silicic acid	0.9 to 2.5 μmol L^{-1}	S. Pickmere (unpublished data)
tCO_2	2060 to 2110 μmol Kg^{-1}	K. Currie (unpublished data)
Dissolved iron	0.12 to 0.07 nmol L^{-1}	Boyd et al. (2005)

Table 3. A summary of the co-variation of physical and biogeochemical property anomalies due to climate change. Each entry in the table reports the linear regression coefficients (slope and correlation coefficient) for the spatial anomalies from the CCSM1.4-carbon simulation for either interannual variability (monthly values from 100 years of control simulation) or anthropogenic climate change (found from differencing the A2 case decadal average maps 2020–2029 minus 2000–2009; Fig. 3). Separate regressions are computed for the subpolar and polar domains. No slope is reported for regressions where the absolute value of the correlation coefficient is less than 0.2.

Interannual Variability		Subpolar		Polar	
X Variable	Y Variable	Slope Y/X	Correlation r	Slope Y/X	Correlation r
T (deg. C)	Hmix (m)	−9.24	−0.33	−5.29	−0.36
T (deg. C)	PO_4(μmol/l)	−0.057	−0.75	−0.054	−0.76
T (deg. C)	Fe (nmol/l)	−0.033	−0.39	−0.036	−0.68
Hmix (m)	PO_4(μmol/l)	0.0014	0.52	0.0028	0.59
Hmix (m)	Fe (nmol/l)	.00067	0.68	0.0028	0.58
Fe (nmol/l)	PO_4(μmol/l)	4.02	0.68	2.33	0.80
Climate Change		Subpolar		Polar	
X Variable	Y Variable	Slope Y/X	Correlation r	Slope Y/X	Correlation r
T (deg. C)	Hmix (m)	n/a	0.11	−8.49	−0.42
T (deg. C)	PO_4(μmol/l)	−0.030	−0.76	−0.030	−0.45
T (deg. C)	Fe (nmol/l)	−0.008	−0.75	−0.086	−0.77
Hmix (m)	PO_4(μmol/l)	n/a	−0.05	0.0016	0.50
Hmix (m)	Fe (nmol/l)	n/a	−0.04	0.0048	0.67
Fe (nmol/l)	PO_4(μmol/l)	4.75	0.76	0.54	0.53

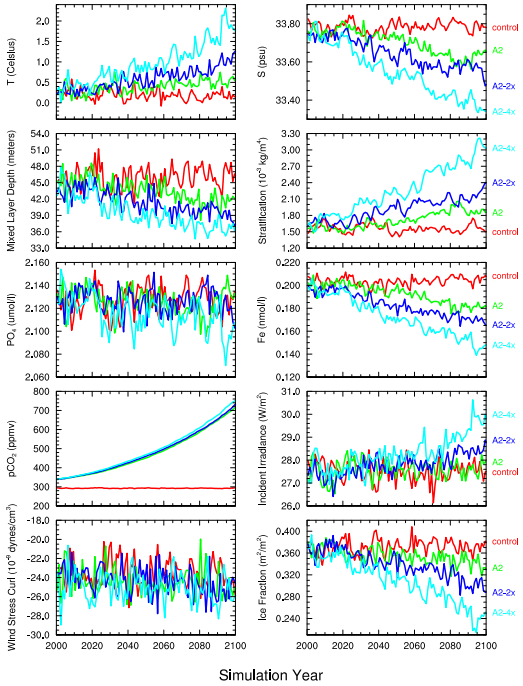

Fig. 1. Annual mean surface water time-series plots (model years 2000–2100) from the control (red) and transient warming simulations (IPCC SRES A2 case green; A2-2x case dark blue; and A2-4x case light blue) averaged over polar waters from the CSM1.4-carbon model. Each panel displays a separate physical or chemical property (temperature, salinity, mixed layer depth, density stratification, phosphate, dissolved iron, pCO_2, incident photosynthetically available radiation, upwelling, and ice fraction). The S. Ocean climate change signals in the transient simulations are approximately (though not exactly) zonal, and the model Southern Ocean is partitioned into polar and subpolar waters based on frontal structure, the boundary being set as the simulated 130 Sv streamfunction that approximates well the boundary between the two water masses.

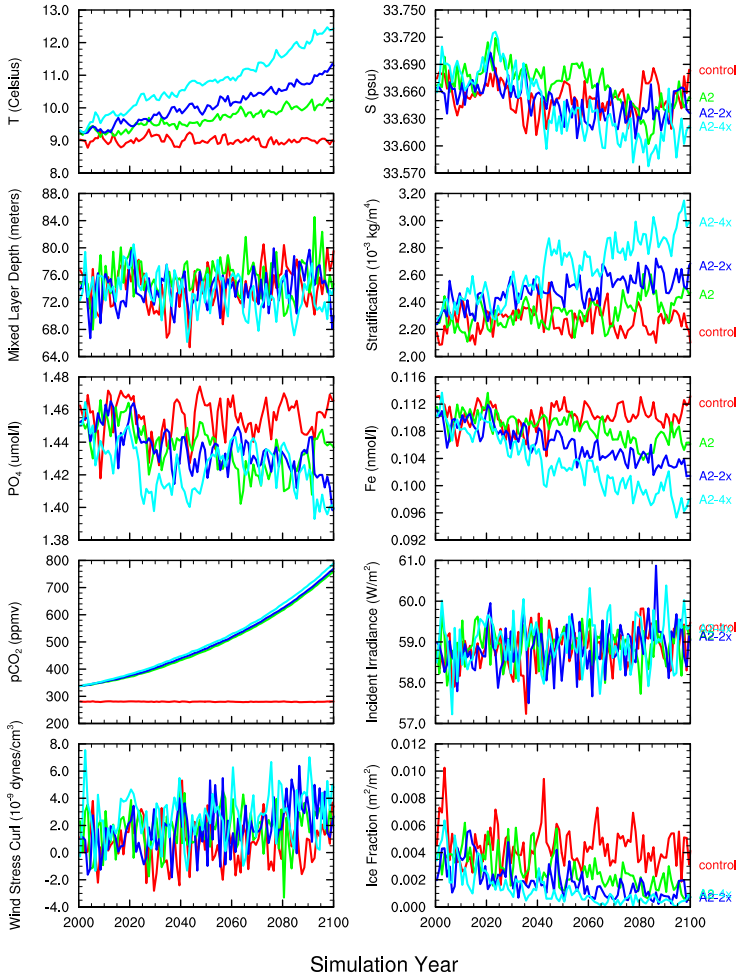

Fig. 2. The same as Fig. 1 but for subpolar waters.

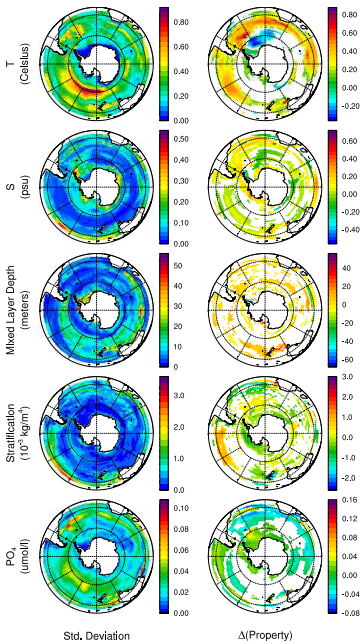

Fig. 3. Spatial maps of S. Ocean interannual variability and anthropogenic climate response from the CSM1.4-carbon transient IPCC SRES A2 simulation. The left column shows the natural interannual variability, expressed as the standard deviation of the annual means from a 10 year segment of the control simulation; the right column shows the climate response expressed as the temporal difference over a 20 year time period, the average of model years 2020–2029 minus the average of model years 2000–2009. Each row displays a separate surface water physical or chemical property (temperature, salinity, mixed layer depth, density stratification, phosphate, dissolved iron, pCO_2, incident photosynthetically available radiation, upwelling, and ice fraction). Regions where the absolute value of the temporal difference is less than one standard error of the difference between the means are masked out.